The Identification of Prognostic and Metastatic Alternative Splicing in Skin Cutaneous Melanoma

Runzhi Huang[1,2,3,*], Mingxiao Li[1,3,*], Zhiwei Zeng[1,3,*], Jie Zhang[3], Dianwen Song[4], Peng Hu[1,2], Penghui Yan[1], Shuyuan Xian[5], Xiaolong Zhu[1,3], Zhengyan Chang[6], Jiayao Zhang[7], Juanru Guo[7], Huabin Yin[4], Tong Meng[4,8], and Zongqiang Huang[1,2]

Abstract

Skin cutaneous melanoma (SKCM) is a type of highly invasive cancer originated from melanocytes. It is reported that aberrant alternative splicing (AS) plays an important role in the neoplasia and metastasis of many types of cancer. Therefore, we investigated whether ASEs of pre-RNA have such an influence on the prognosis of SKCM and the related mechanism of ASEs in SKCM. The RNA-seq data and ASEs data for SKCM patients were obtained from the TCGA and TCGASpliceSeq database. The univariate Cox regression revealed 1265 overall survival-related splicing events (OS-SEs). Screened by Lasso regression, 4 OS-SEs were identified and used to construct an effective prediction model (AUC: .904), whose risk score was proved to be an independent prognostic factor. Furthermore, Kruskal–Wallis test and Mann–Whitney–Wilcoxon test showed that an aberrant splicing type of aminoacyl tRNA synthetase complex-interacting multifunctional protein 2 (AIMP2) regulated by CDC-like kinase 1 (CLK1) was associated with the metastasis and stage of SKCM. Besides, the overlapped signal pathway for AIMP2 was galactose metabolism identified by the co-expression analysis. External database validation also confirmed that AIMP2, CLK1, and the galactose metabolism were associated with the metastasis and stage of SKCM patients. ChIP-seq and ATAC-seq methods further confirmed the transcription regulation of CLK1, AIMP2, and other key genes, whose cellular expression was detected by Single Cell Sequencing. In conclusion, we proposed that CLK1-regulated AIMP2-78704-ES might play a critical role in the tumorigenesis and metastasis of SKCM via galactose metabolism. Besides, we established an effective model with MTMR14-63114-ES, URI1-48867-ES, BATF2-16724-AP, and MED22-88025-AP to predict the metastasis and prognosis of SKCM patients.

[1]Department of Orthopaedics, The First Affiliated Hospital of Zhengzhou University, Zhengzhou, China
[2]Division of Spine, Department of Orthopedics, Tongji Hospital Affiliated to Tongji University School of Medicine, Shanghai, China
[3]Zhengzhou University School of Medicine, Zhengzhou University, Zhengzhou, China
[4]Shanghai First Maternity and Infant Hospital, Tongji University School of Medicine, Shanghai, China
[5]Department of Orthopedics, Shanghai General Hospital, School of Medicine, Shanghai Jiaotong University, Shanghai, China
[6]Tongji University School of Medicine, Shanghai, China
[7]Department of Pathology, Shanghai Tenth People's Hospital, Tongji University School of Medicine, Shanghai, China
[8]Tongji University School of Mathematical Sciences, Tongji University, Shanghai, China
[9]Tongji University Cancer Center, Shanghai Tenth People's Hospital, Tongji University School of Medicine, Shanghai, 200072, China

*Runzhi Huang, Mingxiao Li and Zhiwei Zeng have contributed equally to this work.

Corresponding Authors:
Zongqiang Huang, PhD, Department of Orthopaedics, The First Affiliated Hospital of Zhengzhou University, Zhengzhou 450052, China.
Email: gzhuangzq@163.com

Tong Meng, MD, Tongji University Cancer Center, Shanghai Tenth People's Hospital, Tongji University School of Medicine, 301 Yanchang Road, Shanghai 200072, China.
Email: mengtong@medmail.com.cn

Huabin Yin, MD, Department of Orthopedics, Shanghai General Hospital, School of Medicine, Shanghai Jiaotong University, Shanghai 200080, China.
Email: yinhuabin@aliyun.com

Introduction

Skin cutaneous melanoma (SKCM) is a rare cancer that accounts for 1% of all malignant tumors. Genetically, as an ever-increasing and extremely invasive type of cancer, it is caused by the malignant proliferation of melanocytes.[1-3] Although surgical treatment has been shown to be successful in localized melanoma, SKCM still has a high incidence of local recurrence and distant metastasis.[3,4] As a difficult stage of SKCM, metastatic SKCM often has a poor response to conventional therapies. Although the discovery of BRAF driver mutations and BRAF target inhibitors has significantly improved the prognosis of patients with metastatic melanoma, a considerable number of BRAF wild-type patients with metastatic melanoma were unable to benefit from the new target treatment.[5,6] Furthermore, potential immunotherapies for BRAF wild-type individuals with metastatic SKCM, such as anti-PD-1, anti-CTLA4, and interleukin-2, do not demonstrate a long-term treatment impact.[7,8] As a result, there is an urgent need to investigate the etiology and metastatic mechanisms of SKCM in order to identify novel therapeutic targets for SKCM therapy.

Alternative splicing (AS), an important post-transcriptional regulation process, effectively diversifies the structures and functions of mRNAs produced from a single gene.[9,10] Furthermore, splicing factors (SFs) control alternate splicing events (ASEs), forming a complex regulatory network.[11,12] There are new studies indicating a link between aberrant AS and cancer incidence, development, and resistance to treatment.[13,14] The amount of SF expression has also been shown to affect the splicing patterns of numerous proteins that participate in cancer-related pathways.[15] Hence, we postulated that abnormal ASEs and SFs may serve as critical prognostic indicators and new treatment targets for patients with SKCM.

Although a thorough study of ASEs and a regulatory network of ASEs and SFs has been discovered in melanoma, metastasis-associated ASEs and prognostic signaling pathways, which are equally essential to the prognosis of SKCM, have been overlooked.[16] In the present research, an integrated bioinformatics analysis of AS profiling was conducted to discover the overall survival-associated ASEs (OS-SEs) in patients with SKCM, and a prognostic model was built to predict the survival of patients with SKCM, which may be useful in therapeutic treatment. Furthermore, Pearson correlation analysis revealed metastasis-associated ASEs, as well as regulatory SFs and signaling pathways, to uncover the underlying metastasis mechanism of SKCM, which may offer prospective biomarkers and therapeutic targets for SKCM metastasis.

Material and Methods

Data Collection

RNA sequencing data and clinical information of 262 SKCM patients were obtained from the Cancer Genome Atlas (TCGA) Database (https://tcgadata.nci.nih.gov/tcga/). Meanwhile, the gene expression level of 390 alternative SFs was extracted from the 262 patients' RNA-seq data. The percent Spliced In (PSI) value was also imputed for seven kinds of AS events to quantify AS events.

Identification of OS-SEs

The univariate Cox model was applied to identify OS-SEs, which were illustrated in the UpSet plots. In addition, the prognosis-associated ASEs and prognosis-unassociated ASEs were both integrated in the volcano plot. Meanwhile, we selected the top 20 OS-SEs of alternative promoter (AP), exon skip (ES), alternative acceptor site (AA), mutex exon (ME), alternative terminator (AT), reserved intron (RI), and alternative donor site (AD) to show in the seven bubble plots, respectively, where the size and color of bubbles signified the value of these ASEs for overall survival (OS).

Construction of Prognostic Model

Before the multivariate Cox regression, Lasso regression was applied to screen the top 20 prognostic-associated OS-SEs to avoid overfitting of the prediction model. Then, the regression coefficient of each prognostic factor screened by Lasso regression was determined by the multivariate Cox regression, represented by β value. Thus, risk score could be obtained by the following formula

$$\sum_{i=1}^{n} \beta i \times PSI$$

The area under ROC curve was applied to test the accuracy of the model. Based on the median value, the samples were clustered into two risk subgroups medially. Then, Kaplan–Meier survival analysis was performed to show the difference between the high- and low-risk subgroups. In addition, these patients were listed in ascending order by risk score to make the risk curve, scatter plot, and heatmap. The univariate and multivariate Cox regression analyses were performed to test whether the risk score was able to predict the survival probability independently, together with age, sex, grade, stage, and TNM stage.
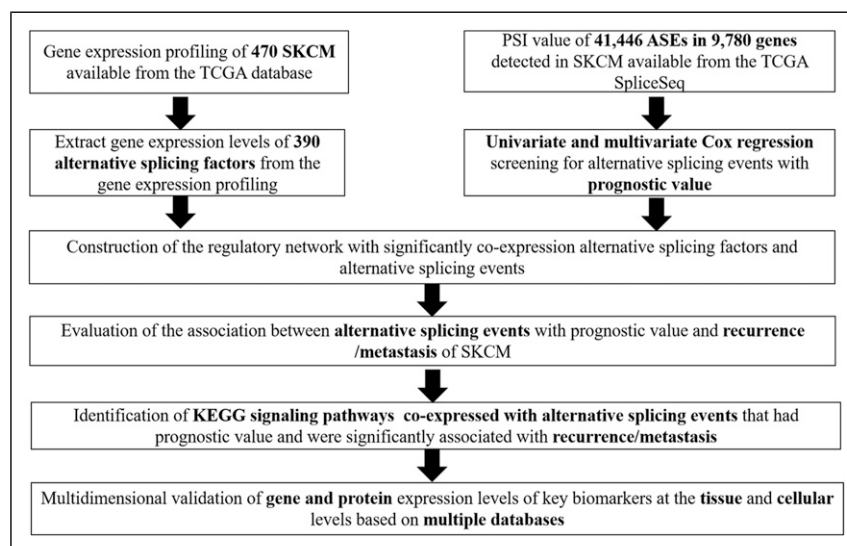
Figure 1. The flowchart of analysis process.

Construction of Splicing Correlation Network

Pearson correlation analysis was implemented to explore the possible correlation and interaction between OS-SEs and 390 SFs retrieved in the SpliceAid2 database. After excluding regulation couples with P > .001 and the absolute value of correlation coefficient <.750, the regulation network was produced by Cytoscape (3.7.1).[17] In the network plot, SF and OS-SEs were represented by arrows and ellipses, respectively. Similarly, high and low risks of OS-SEs were defined as red and purple, respectively. Positive and negative regulations were symbolized by red and green, respectively.

We also performed Kruskal–Wallis test and Mann–Whitney–Wilcoxon test to search the OS-SEs associated with metastasis and/or TNM stage, and the results were shown in the beeswarm plots. The Venn plot was also produced to show the intersections between metastasis-related OS-SEs and stage-related OS-SEs.

Signaling Pathways Enrichment Analysis

First, we used Gene Set Variation Analysis (GSVA) to identify the signaling pathways related with prognosis. The univariate Cox analysis was then used to filter the OS-related signaling pathways. The metastatic and stage-related OS-SE, as well as the prognosis-related Kyoto encyclopedia of Genes and Genomes (KEGG) pathways, were co-expressed to discover potential downstream processes of specific OS-SE.

Online Database Validation

In order to eliminate possible bias, we also collected and analyzed the gene and protein expression levels of major biomarkers in tissues in many databases, including the human

protein atlas,[18] GEPIA,[19] UCSC xena,[20] UALCAN,[21] cBio-portal,[22] Oncomine,[23] CCLE,[24] STRING, and Pathcard.

Assay for Transposase-Accessible Chromatin using Sequencing (ATAC-seq) and Chromatin Immunoprecipitation sequencing (ChIP-seq)

In order to further validate the transcriptional regulation of CLK1, and other key genes (BATF2, MED22, MTMR14, and URI1), ATAC-seq and ChIP-seq were performed. First, the ATAC-seq data of SKCM patients were acquired from the TCGA database, which was used to detect the chromatin accessibility in the position of key genes. Furthermore, we tested the binding relationship between CLK1 and key genes directly using the ChIP-seq method, which utilized the Cistrome database.[25,26]

Single Cell Sequencing

We acquired the Single Cell Sequencing data of melanoma from Single Cell Expression Atlas and analyzed the expression of these key genes in cellular level, aiming at discovering potential cellular mechanism.[27]

Statistics Analysis

In this study, we used the R software (www.r-project.org; version 3.6.1; Institute for Statistics and Mathematics, Vienna, Austria) across all statistical analyses (two-sided P value <.05 was pre-set as statistically significant).

Results

Identification of ASEs in SKCM

The flow chart illustrated the analysis process of this study (Figure 1). Supplementary Table S1 summarizes the
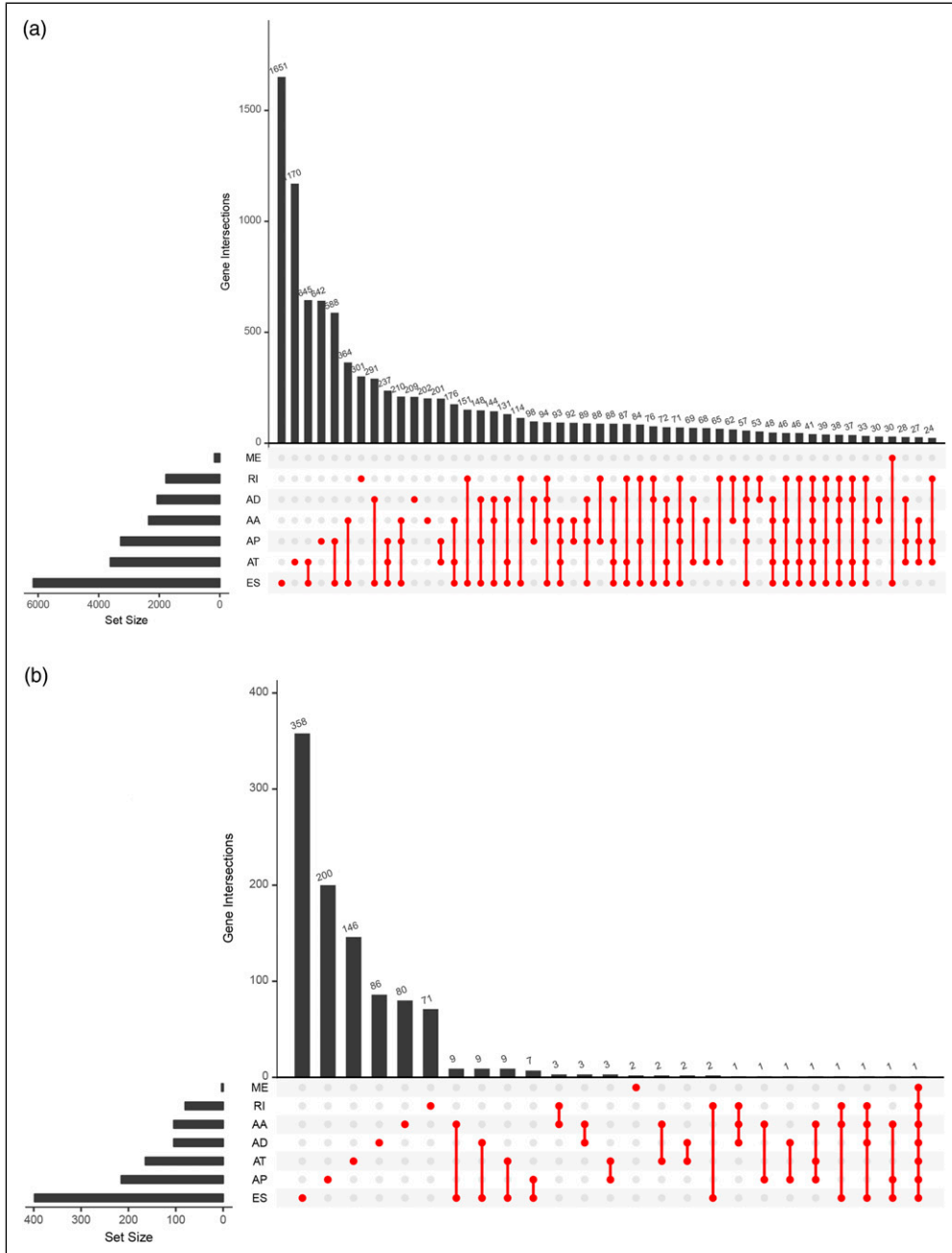
Figure 2. The Upset plot of different types of ASEs in the SKCM patients derived from TCGA database (A). The Upset plot of seven types of ASEs which are associated with overall survival of SKCM (B). SKCM: Skin cutaneous melanoma; TCGA: the Cancer Genome Atlas; ASEs: alternative splicing events.

baseline information of 470 patients diagnosed with SKCM. A total of 470 SKCM patient's data have been identified from the TCGA database to analyze ASEs. Among these SKCM cases, a total of 41 446 ASEs in 9780 genes were identified, including 2350 AAs (202 genes), 2069 ADs (209 genes), 3273 APs (642 genes), 3614 ATs (1170 genes), 6160 ESs (1651 genes), 175 MEs (30 genes), and 1780 RIs (301 genes) (Figure 2A). Therefore, an individual gene was able to go through various types of

splicing events. Obviously, ES was the most prominent splicing pattern.

Identification of OS-SEs

According to results of the univariate Cox regression analysis, a total of 1265 ASEs were significantly related to OS, which was integrally illustrated in the Upset plot (Figure 2B). Meanwhile, the volcano plot revealed that most of the ASEs
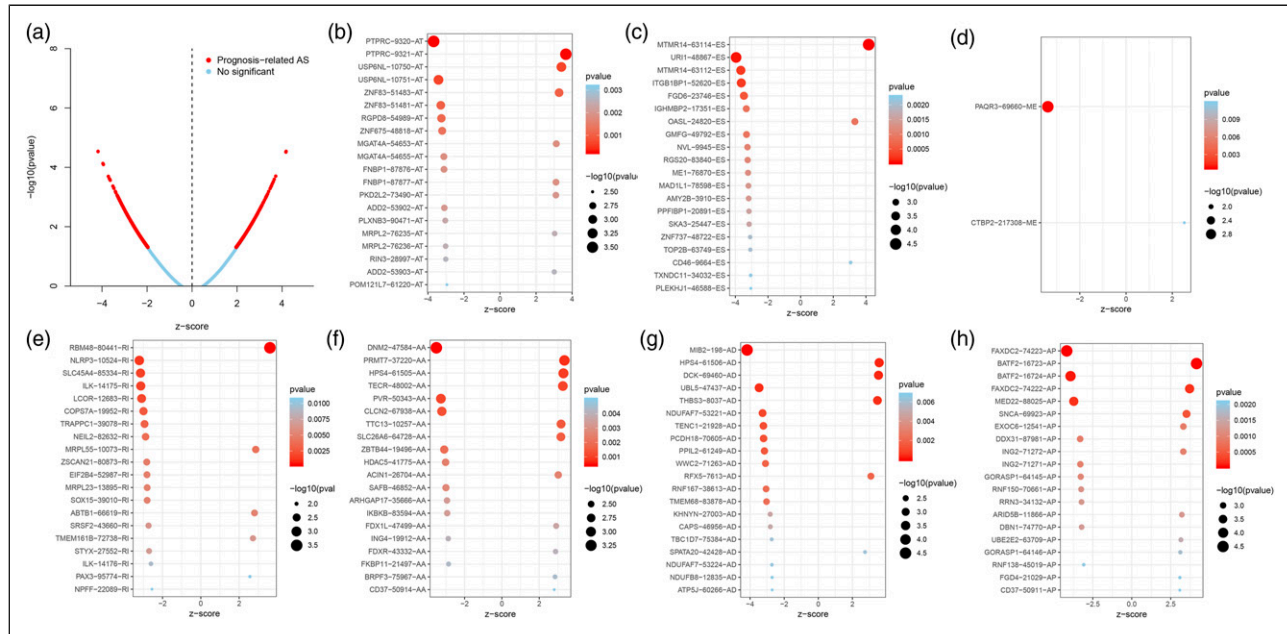
Figure 3. The volcano plot of prognosis-related ASEs in SKCM (A). The bubble plot of the top 20 OS-ASEs in seven types of alternative splicing (C-G). ASEs: alternative splicing events. SKCM: Skin cutaneous melanoma; ASEs: alternative splicing events.

were prognosis-related in SKCM (Figure 3A). The bubble plots reported the top 20 OS-ASEs of the seven kinds of splicing patterns (Figure 3B-H). Notably, MTMR14-63114-ES, URI1-48867-ES, BATF2-16724-AP, and MED22-88025-AP were among the most significant differentially expressed OS-SEs in patients with SKCM.

Construction of Prognostic Model for SKCM

To avoid over-fitting of the model, we implemented the Lasso regression to further screen the top 20 OS-SEs (Figures 4A and 4B). The result indicated that MTMR14-63114-ES, URI1-48867-ES, BATF2-16724-AP, and MED22-88025-AP were the most significant prognostic biomarkers. Based on the four biomarkers, we performed the multivariate Cox regression analysis to identify the value of the individual OS-SEs on the OS in patients with SKCM and constructed the corresponding predict model, whose accuracy and reliability were proved by ROC curve (AUC:0.788) (Figure 4C). Then, the risk score of each sample was obtained according to the prognosis model, with a median level of 7.168213949. The Kaplan–Meier plot indicated that there was an obvious difference in survival probability between the high- and low-risk subgroups, indicating the effectiveness of this predict model (Figure 4D). Besides, the risk curve and scatter plot showed that patients with a higher risk score tended to live longer, which also supported the validity of the model (Figures 4E and 4F). In addition, the heatmap was used to compare the expression level of OS-SEs integrated in the multivariate Cox regression. In the heatmap, MTMR14-63114-ES was lowly expressed, while URI1-48867-ES, BATF2-16724-AP, and MED22-88025-AP were highly expressed in patients with higher risk score (Figure 4G).

Validation of Risk Score as an Independent Prognostic Analysis

Next, the univariate and multivariate Cox regression were applied to evaluate the independent prognostic value of risk score, together with other clinical parameters, including age, gender, grade, stage, and TNM stage. The hazard ratio in the univariate (HR = 1.060, 95%CI (1.035–1.086), $P < .001$) and multivariate Cox regression (HR = 1.065, 95%CI (1.029–1.103), $P < .001$) analyses justified that the risk score could be regarded as the independent predictor (Figure 5).

Correlation of OS-SEs and SF Expression

With regard to the regulatory SF of aminoacyl tRNA synthetase complex-interacting multifunctional protein 2 (AIMP2)-78704-ES, the network plot indicated that AIMP2-78704-ES (the high risk OS-SE, red ellipse) was regulated positively (red lines) by both CDC2-like kinase 1 (CLK1) and SRSF11 (Figure 6A). To explore the OS-SEs related to both nodal and distant metastases, we performed univariate Cox analysis and created a Venn plot to illustrate the overall results, indicating that AIMP2-78704-ES was the only OS-SEs reaching the screening standard (Figures 6B-6D).

Comprehensive Analysis of ASEs and Signaling Pathways

The results of the GSVA and the univariate Cox regression analysis showed that a total of 185 KEGG pathways were related to OS. Then, the Pearson correlation analysis between AIMP2-78704-ES and all the OS-related KEGG pathways
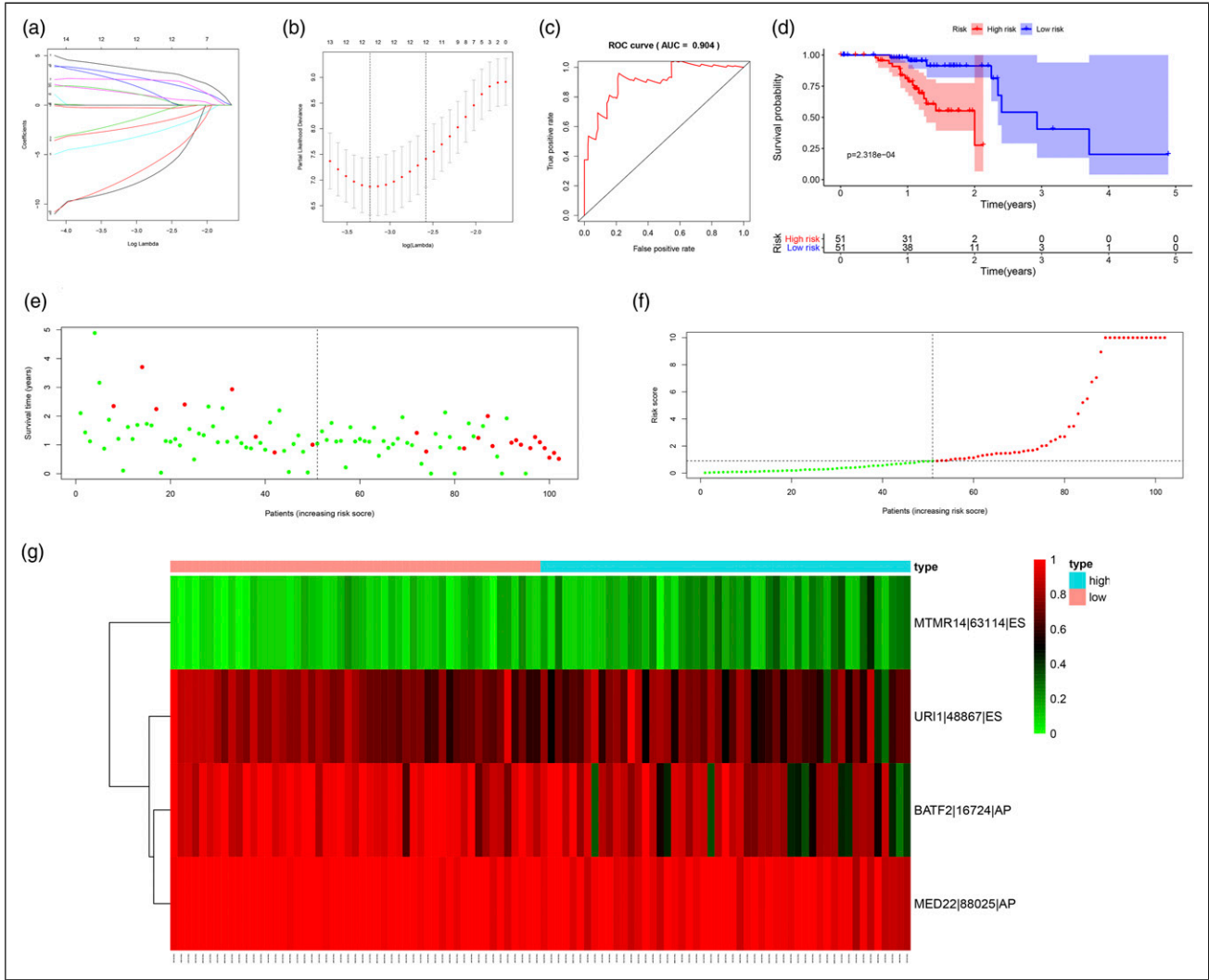
Figure 4. The multivariate Cox regression model was based on ASEs selected by Lasso regression (A, B). The multivariate Cox regression model was proved to be reliable by ROC curve (AUC:0.788) (C) According to the predict model, the high-risk group in this predict model was shown to have larger survival probability (D), longer survival time (E), and mortality (F) than low-risk group. Among the four ASEs integrated in the model, MTMR14-63114-ES happened more frequently, but URI1-48867-ES, BATF2-16724-AP, and MED22-88025-AP happened less frequently in high-risk group (G).
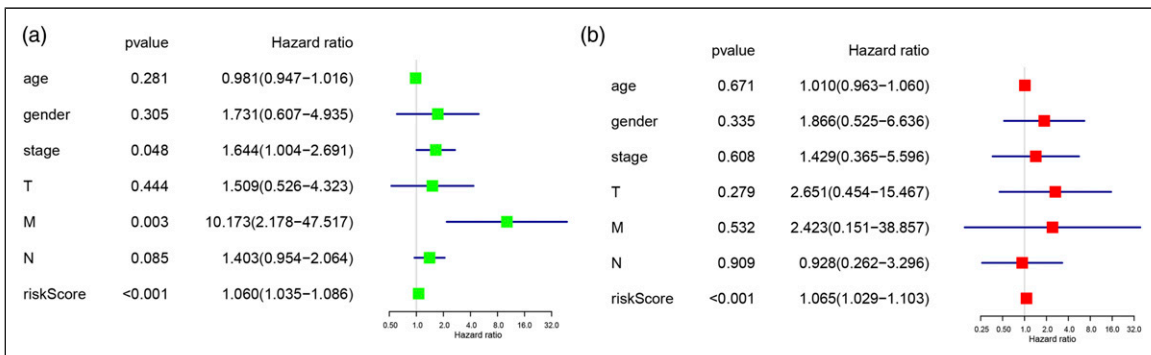

Figure 5. In the independent prognostic factor test, the hazard ratios of risk score in the univariate and multivariate Cox regression analyses were (HR = 1.060, 95%CI(1.035–1.086), *P* < .001) (A) and (HR = 1.065, 95%CI(1.029–1.103), *P* < .001) (B), respectively.
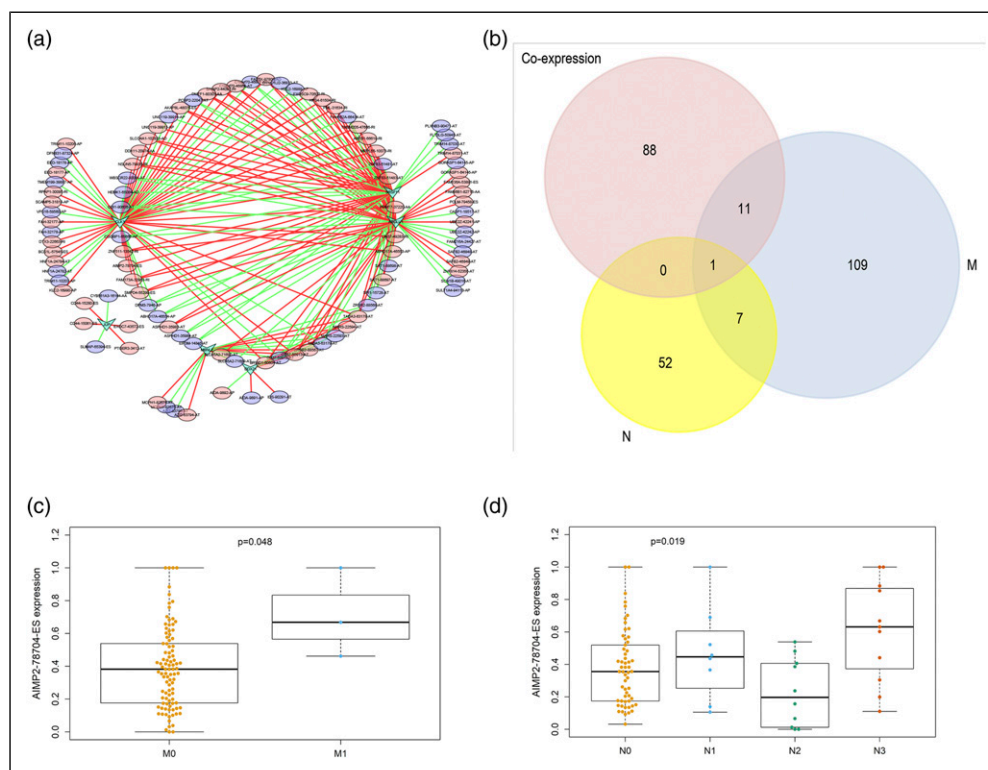
Figure 6. The splicing correlation network in SKCM (A) SF and OS-SEs were represented by arrows and ellipses separately. Similarly, high- and low-risk of OS-SEs were defined as red and purple and positive and negative regulations were symbolized by red and green, respectively. With the result of Kruskal–Wallis test and Mann–Whitney–Wilcoxon test (C, D), AIMP2-78704-ES was identified as the only ASE associated with both metastasis and TNM stage in the Venn plot (B). SKCM: Skin cutaneous melanoma; ASEs: alternative splicing events.

was performed to search for their co-expression association. The results revealed that AIMP2-78704-ES was significantly correlated with the galactose metabolism pathway ($R = -.41$, $P < .001$) (Figure 7).

External Validation

To decrease bias induced by limited samples and vacant experimentally mechanism evidence, we used multiple online database to strength the reliability of our bioinformatics analysis. First, protein–protein interaction (PPI) network retrieved from Pathcard database suggested that Glucose-6-Phosphate Isomerase (GPI), Hexokinase 3 (HK3), Glycogen Synthase 1 (GYS1), Glucose-6-Phosphatase Catalytic Subunit 3 (G6PC3), and Beta-1,4-Galactosyltransferase 2 (B4GALT2) were the key members in galactose metabolism pathway (Supplementary Figure S1A). Besides, STRING database showed that CLK1 and AIMP2 were closed connected via galactose metabolism pathway (Supplementary Figure S1B). Then, Oncomine database illustrated that AIMP2, GPI, HK, GYS1, and G6PC3 were differentially expressed between SKCM and normal tissues (Supplementary Figure S2). CCLE and the human protein atlas provided the evidence from the aspect of cell lines and protein (Supplementary

Figures S3 and S4). UALCAN database showed that CLK1, HK3, and G6PC3 were differentially expressed between localized and metastatic tumor (Supplementary Figures S5A-S5C), and that AIMP2, GPI, HK3, GYS1, G6PC3, and B4GALT2 were significantly related to OS (Supplementary Figures S5D-S5I). The expression heatmap provided by UCSC Xena uncovered the relationship between the expression of key biomarkers and OS (Supplementary Figure S6A). Besides, AIMP2, GPI, HK3, and B4GALT2 were found significantly related to patients' OS (Supplementary Figure S6). Validation from GEPIA suggested that CLK1, GPI, HK3, and G6PC3 were differentially expressed between normal and cancer cells (Supplementary Figure S7). Ultimately, both GEPIA and cBioportal illustrated the close correlation between AIMP and other key biomarkers, and the relationship between gene expression and patients' OS (Supplementary Figures S7 and S8). Supplementary Table S2 summarizes of multidimensional external validation results base on multiple databases

ATAC-Seq and ChIP-Seq Verification

ATAC-seq and ChIP-seq methods were utilized to verify the transcription regulation between CLK1 and key genes in the
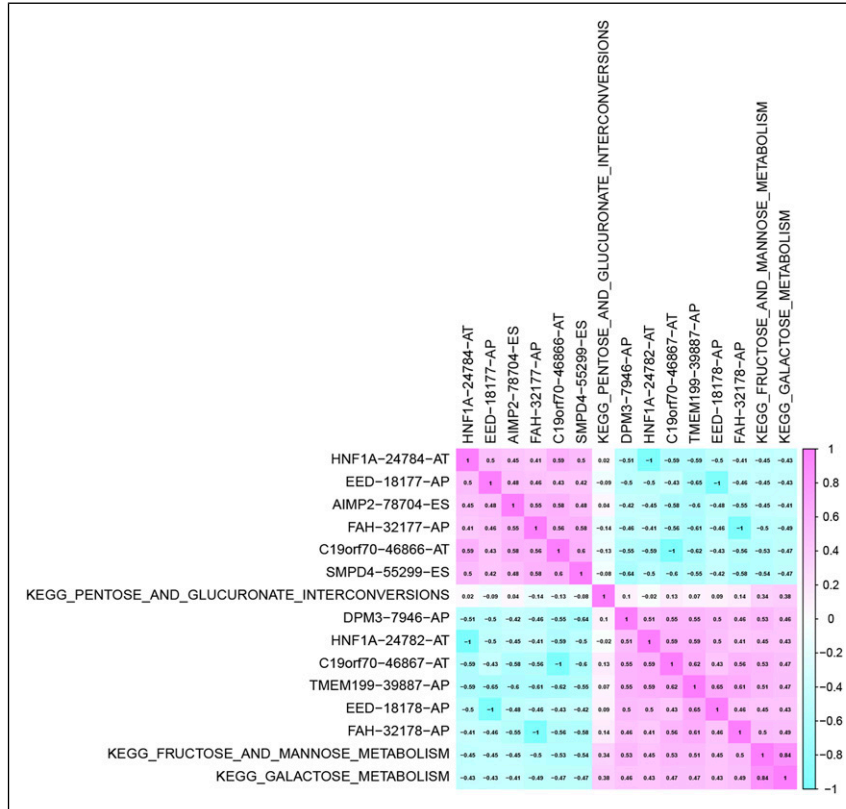
Figure 7. Galactose metabolism pathways were found to be correlated with AIMP2-78704-ES.

study. The results of ATAC-seq indicated that the chromatin regions in the locations of CLK1, AIMP2, BATF2, MED22, MTMR14, and URI1 were open and accessible (Supplementary Figure S9). In addition, the ChIP-seq data retrieved from the Cistrome database further revealed the DNA fragments binding with CLK1 in mouse model. The results reported strong binding peaks in the location of AIMP2, BATF2, MED22, MTMR14, and URI1 (Supplementary Figure S10). Overall, ATAC-seq and ChIP-seq together validated the binding relationship of CLK1 and other key genes in chromosomal level.

Single Cell Sequencing Verification

In order to discover the cellular expression of these key biomarkers, we analyzed the single cell sequencing data of melanoma obtained from Single Cell Expression Atlas and detected the expression of AIMP2, CLK1, BATF2, MED22, MTMR14, and URI1 (Supplementary Figures S11A and S11B) in cellular level. The results revealed that AIMP2 was highly expressed in cancer-associated fibroblasts and tumor endothelial cells, and CLK1 was highly expressed in lymph node T cells, tumor T cells, and B cell. (Supplementary Figures S11C and S11D). The cellular expression of BATF2, MED22, MTMR14, and URI1 was also reported by

Single Cell Sequencing method (Supplementary Figures S11E-S11H).

Discussion

SKCM, as a highly invasive cancer, has been increasingly escalated lately.[28,29] Multiple studies revealed that the prognosis of SKCM patients was closely associated with distant metastasis, and those with three or more metastatic sites usually died within one year.[30] Although multidisciplinary therapies were proposed to improve the OS of melanoma patients, most patients with metastatic SKCM still had limited efficacy.[31] Recently, many studies revealed that AS and SFs played important roles in cancer biology and had the potentials to act as the prognostic signature for tumor progression.[10,11,32] However, how AS and SFs functioned in the tumorigenesis, progression, and metastasis of SKCM was still unclear. In the present study, we found out that regulatory mechanism between AIMP2-78704-ES and its critical SF (CLK1) was actively involved in tumor metastasis and TNM stage.

CLK1, composed of 454 amino acids, can autophosphorylate on serine, tyrosine, and threonine residues and phosphorylate exogenous substrates on serine and threonine residues.[33] AS was regulated by SFs whose activity was in turn regulated by phosphatases and splice factor

kinases.[34,35] Without exception, CLK1 phosphorylation of serine/arginine-rich proteins was also proved to be central to RNA splicing reactions, and actively got involved in a myriad of normal physiology and diseases, including cancer.[36,37] Yuying Liu et al[38] found that phosphorylation regulation of CLK1 on eight serine residues of alternative splicing factor 45 (SPF45) was positively correlated with enhanced cell migration and invasion capability of ovarian cancer cells. In addition, the expression of CLK1 could also be induced by hypoxia in prostate cancer cells PC3.[39] In our study, we discovered that CLK1 could regulate the pre-mRNA splicing of AIMP2 to promote metastasis in patients with SKCM, which was in high accordance with the previous studies. Therefore, the inhibition of CLK1 may become a novel therapeutic target for cancer by selectively reducing some cancer-relevant proteins.[40]

AIMP2 was a cytoplasmic protein acting as a non-enzymatic scaffold factor of the multi-tRNA synthetase complex (MSC), which was required for assembly and stability of the complex.[41,42] Previous studies showed that AIMP2 might serve as an important molecule in regulating cell proliferation and apoptosis after DNA damage through interacting with p53.[41,43] Moreover, AIMP2-DX2, one of variant splicing isoform of AIMP, was significantly associated with the tumorigenesis, cancer cell proliferation, invasion, and migration in many cancers, including lung cancer, ovarian cancer, and nasopharyngeal carcinoma[44-47] In the study of Yin K et al, elevating the expression of AIMP2 splicing variation could shorten the survival of patients with tongue squamous cell carcinoma, which was also in high accordance with our study.[48] Taken together, AIMP2 may also serve as a novel therapeutic target of SKCM.

To further investigate the mechanisms of CLK1 in regulating AIMP2-78704-ES, we performed the Pearson correlation analysis between OS-related KEGG signaling pathways and AIMP2-78704-ES, and found out that abnormal ASE of AIMP2 might influence patients' prognosis via galactose metabolism pathway. Galactose was a natural aldohexose usually presenting in the form of D-configuration. It was known that D-galactose was a common substance in bacteria, plants, and animals, and that galactose was metabolized through the Leloir pathway, which required a close cooperation of multiple metabolic enzymes.[49] The mis-regulation or malfunction of any component of metabolism pathway could result in the accumulation of toxic intermediate products and damage to cells.[50] Through PPI network of galactose metabolism retrieved from Pathcard database, we found out that Glucose-6-Phosphate Isomerase (GPI), Hexokinase 3 (HK3), Glycogen Synthase 1 (GYS1), Glucose-6-Phosphatase Catalytic Subunit 3 (G6PC3), and Beta-1,4-Galactosyltransferase 2 (B4GALT2) were the key members in the galactose metabolism pathway. A myriad of studies have uncovered the function of these 5 key biomarkers in tumorigenesis, progression, invasion, and migration.[51,52] Moreover, through multiple dimensions validation from different online databases, we also found out that GPI, HKS, GYS1, G6PC3, and

B4GALT2 were significantly related to OS in patients with SKCM, and these biomarkers were also greatly correlated with AIMP2, indicating the reliable analysis of our study.[53,54]

Despite the thorough bioinformatics analysis, our research has several limitations. First, the sample information and sequencing data were mainly acquired from Western authorities, leaving adequate information on Asian individuals unfilled. Second, although we utilized several databases to identify gene and protein expression levels of important biomarkers at the tissue and cellular levels to reduce bias (Supplementary Figures S1-S8), this was a correlation research from many dimensions rather than a biological mechanism study with exact experiment. Despite its limitations, this research did build an efficient model to predict SKCM patient survival based on four major OS-SEs and concluded that the mechanism of CLK1 in regulating AIMP2-78704-ES may play an essential role in SKCM metastasis. Importantly, in order to further investigate the relevant molecular process and validate our theory, we will conduct rigorous cell, animal, and clinical studies in the future.

Conclusion

We established an effective model with MTMR14-63114-ES, URI1-48867-ES, BATF2-16724-AP, and MED22-88025-AP to predict the metastasis and prognosis of SKCM patients. Through the bioinformatics analysis, we discovered that CLK1 might regulate AIMP2-78704-ES via galactose metabolism pathway in tumorigenesis, metastasis, and poor clinical outcomes of patients with SKCM.

Author Contributions

Conception/design: Runzhi Huang, Mingxiao Li, Zhiwei Zeng, Jie Zhang, Dianwen Song, Peng Hu, Penghui Yan, Shuyuan Xian, Xiaolong Zhu, Zhengyan Chang, Jiayao Zhang, Juanru Guo, Huabin Yin, Tong Meng, and Zongqiang Huang
Collection and/or assembly of data: Runzhi Huang, Mingxiao Li, Zhiwei Zeng, Jie Zhang, Dianwen Song, Peng Hu, Penghui Yan, Shuyuan Xian, Xiaolong Zhu, Zhengyan Chang, Jiayao Zhang, and Juanru Guo
Data analysis and interpretation: Runzhi Huang, Mingxiao Li, Zhiwei Zeng, Jie Zhang, Dianwen Song, Peng Hu, Penghui Yan, Shuyuan Xian, Xiaolong Zhu, Zhengyan Chang, Jiayao Zhang, Juanru Guo, Huabin Yin, Tong Meng, and Zongqiang Huang
Manuscript writing: Runzhi Huang, Mingxiao Li, Zhiwei Zeng, Jie Zhang, Dianwen Song, Peng Hu, Penghui Yan, Shuyuan Xian, Xiaolong Zhu, Zhengyan Chang, Jiayao Zhang, Juanru Guo, Huabin Yin, Tong Meng, and Zongqiang Huang Final approval of manuscript: Runzhi Huang, Mingxiao Li, Zhiwei Zeng, Jie Zhang, Dianwen Song, Peng Hu, Penghui Yan, Shuyuan Xian, Xiaolong Zhu,

Zhengyan Chang, Jiayao Zhang, Juanru Guo, Huabin Yin, Tong Meng, and Zongqiang Huang

Declaration of Conflicting Interests

The author(s) declared no potential conflicts of interest with respect to the research, authorship, and/or publication of this article.

Funding

Ethics Approval

The study was approved by the Ethics Committee of the First Affiliated Hospital of Zhengzhou University (approval no. 2020-KY-190a).

Informed Consent

All patients provided written informed consent prior to enrollment in the study.

Data Availability

The datasets generated and/or analyzed during the current study are available in the Supplementary Material and TCGA-SKCM program (https://portal.gdc.cancer.gov).

ORCID iD

Zongqiang Huang ⓘ https://orcid.org/0000-0002-2787-1629

Supplementary Material

Supplementary material for this article is available online.

References

1. Koh HK. Cutaneous melanoma. *N Engl J Med*. 1991;325(3): 171-182.
2. Thompson JF, Scolyer RA, Kefford RF. Cutaneous melanoma. *Lancet*. 2005;365(9460):687-701.
3. Coricovac D, Dehelean C, Moaca EA, et al. Cutaneous melanoma-a long road from experimental models to clinical outcome: a review. *Int J Mol Sci*. 2018;19(6).
4. Long GV, Gasal E, Hauschild A. Estimation of distant metastasis-free survival in trials of adjuvant therapy for melanoma. Reply. *N Engl J Med*. 2019;380(14):1376-1377.
5. Seth R, Messersmith H, Kaur V, et al. Systemic Therapy for Melanoma: ASCO Guideline. *J Clin Oncol*. 2020;38(33): 3947-3970.
6. Franken MG, Leeneman B, Gheorghe M, Uyl-de Groot CA, Haanen JBAG, van Baal PHM. A systematic literature review and network meta-analysis of effectiveness and safety outcomes in advanced melanoma. *Eur J Cancer* 1990;123:58-71
7. Luke JJ, Flaherty KT, Ribas A, Long GV. Targeted agents and immunotherapies: optimizing outcomes in melanoma. *Nat Rev Clin Oncol*. 2017;14(8):463-482.
8. Rodríguez-Cerdeira C, Carnero Gregorio M, López-Barcenas A, et al. *Advances in Immunotherapy for Melanoma: A Comprehensive Review*. Mediators of inflammation; 2017:3264217.
9. Baralle FE, Giudice J. Alternative splicing as a regulator of development and tissue identity. *Nat Rev Mol Cell Biol*. 2017; 18(7):437-451.
10. Climente-González H, Porta-Pardo E, Godzik A, Eyras E. The functional impact of alternative splicing in cancer. *Cell Reports*. 2017;20(9):2215-2226.
11. Lee Y, Rio DC. Mechanisms and regulation of alternative pre-mRNA Splicing. *Annu Rev Biochem*. 2015;84:291-323.
12. Urbanski LM, Leclair N, Anczuków O. Alternative-splicing defects in cancer: Splicing regulators and their downstream targets, guiding the way to novel cancer therapeutics. *Wiley Interdisciplinary Reviews: RNA*. 2018;9(4):e1476.
13. Lee SC-W, Abdel-Wahab O. Therapeutic targeting of splicing in cancer. *Nat Med*. 2016;22(9):976-986.
14. Sveen A, Kilpinen S, Ruusulehto A, Lothe RA, Skotheim RI. Aberrant RNA splicing in cancer; expression changes and driver mutations of splicing factor genes. *Oncogene*. 2016;35(19): 2413-2427.
15. David CJ, Manley JL. Alternative pre-mRNA splicing regulation in cancer: pathways and programs unhinged. *Gene Dev*. 2010;24(21):2343-2364.
16. Ma FC, He RQ, Lin P, et al. Profiling of prognostic alternative splicing in melanoma. *Oncology letters*. 2019;18(2):1081-1088.
17. The TCGA Legacy. *Cell*, 2018. 173(2): p. 281-282.
18. Hutter C, Zenklusen JC. The cancer genome atlas: creating lasting value beyond its data. *Cell*. 2018;173(2):283-285.
19. Ryan M, Wong WC, Brown R, et al. TCGASpliceSeq a compendium of alternative mRNA splicing in cancer. *Nucleic Acids Res*. 2016;44(D1):D1018-D1022.
20. Shannon P, Markiel A, Ozier O, et al., Cytoscape: a software environment for integrated models of biomolecular interaction networks. *Genome Research*. 2003;13(11):2498-2504.
21. Tang Z, Li C, Kang B, Gao G, Li C, Zhang Z. GEPIA: a web server for cancer and normal gene expression profiling and interactive analyses. *Nucleic Acids Res*. 2017;45(W1):W98.
22. Goldman M, Craft B, Swatloski T, et al. The UCSC cancer genomics browser: update 2015. *Nucleic Acids Res*. 2015;43: D812-D817.(Database issue)
23. Aguirre-Gamboa R, Gomez-Rueda H, Martínez-Ledesma E, et al. SurvExpress: an online biomarker validation tool and database for cancer gene expression data using survival analysis. *PLoS One*. 2013;8(9):e74250.
24. Cerami E, Gao J, Dogrusoz U, et al. The cbio cancer genomics portal: an open platform for exploring multidimensional cancer genomics data: figure 1. *Cancer Discovery*. 2012;2(5):401-404.

25. Menet JS, Pescatore S, Rosbash M. CLOCK:BMAL1 is a pioneer-like transcription factor. *Genes Dev*. 2014;28(1):8-13.

26. Menet JS, Rodriguez J, Abruzzi KC, Rosbash M. Nascent-Seq reveals novel features of mouse circadian transcriptional regulation. *eLife*. 2012;1:e00011.

27. Tirosh I, Izar B, Prakadan SM, et al. Dissecting the multicellular ecosystem of metastatic melanoma by single-cell RNA-seq. *Science*. 2016;352(6282):189-196.

28. Leonardi GC, Falzone L, Salemi R, et al. Cutaneous melanoma: From pathogenesis to therapy (Review). *Int J Oncol*. 2018; 52(4):1071-1080.

29. Damsky WE, Theodosakis N, Bosenberg M. Melanoma metastasis: new concepts and evolving paradigms. *Oncogene*. 2014;33(19):2413-2422.

30. Chapman PB, Hauschild A, Robert C, et al. Improved survival with vemurafenib in melanoma with BRAF V600E mutation. *N Engl J Med*. 2011;364(26):2507-2516.

31. Robert C, Karaszewska B, Schachter J, et al. Improved overall survival in melanoma with combined dabrafenib and trametinib. *N Engl J Med*. 2015;372(1):30-39.

32. Trincado JL, Sebestyén E, Pagés A, Eyras E. The prognostic potential of alternative transcript isoforms across human tumors. *Genome Medicine*. 2016;8(1):85.

33. Xie SH, Li JQ, Chen YS, Gao P, Zhang H, Li ZY. Molecular cloning, expression, and chromosomal mapping of the porcine CDC-2-like kinase 1 (CLK1) gene. *Biochem Genet*. 2009;47(3-4):266-275.

34. Lev Maor G, Yearim A, Ast G. The alternative role of DNA methylation in splicing regulation. *Trends Genet*. 2015;31(5): 274-280.

35. Czubaty A, Piekiełko-Witkowska A. Protein kinases that phosphorylate splicing factors: Roles in cancer development, progression and possible therapeutic options. *Int J Biochem Cell Biol*. 2017;91(Pt B):102-115.

36. Jain P, Karthikeyan C, Moorthy NS, Waiker D, Jain A, Trivedi P. Human CDC2-like kinase 1 (CLK1): a novel target for Alzheimer's disease. *Curr Drug Targets*. 2014;15(5):539-550.

37. Aubol BE, Wu G, Keshwani MM, et al. Release of SR Proteins from CLK1 by SRPK1: a symbiotic kinase system for phosphorylation control of pre-mRNA splicing. *Mol Cell*. 2016; 63(2):218-228.

38. Liu Y, Conaway L, Rutherford Bethard J, et al. Phosphorylation of the alternative mRNA splicing factor 45 (SPF45) by Clk1 regulates its splice site utilization, cell migration and invasion. *Nucleic Acids Res*. 2013;41(9):4949-4962.

39. Bowler E, Porazinski S, Uzor S, et al. Hypoxia leads to significant changes in alternative splicing and elevated expression of CLK splice factor kinases in PC3 prostate cancer cells. *BMC Cancer*. 2018;18(1):355.

40. ElHady AK, Abdel-Halim M, Abadi AH, Engel M. Development of Selective Clk1 and -4 inhibitors for cellular depletion of cancer-relevant proteins. *J Med Chem*. 2017;60(13):5377-5391.

41. Han JM, Park B-J, Park SG, et al. AIMP2/p38, the scaffold for the multi-tRNA synthetase complex, responds to genotoxic stresses via p53. *Proc Natl Acad Sci Unit States Am*. 2008; 105(32):11206-11211.

42. Schwarz MA, Lee DD, Bartlett S. Aminoacyl tRNA synthetase complex interacting multifunctional protein 1 simultaneously binds Glutamyl-Prolyl-tRNA synthetase and scaffold protein aminoacyl tRNA synthetase complex interacting multifunctional protein 3 of the multi-tRNA synthetase complex. *Int J Biochem Cell Biol*. 2018;99:197-202.

43. Choi JW, Kim DG, Park MC, et al. AIMP2 promotes TNFalpha-dependent apoptosis via ubiquitin-mediated degradation of TRAF2. *J Cell Sci*. 2009;122(Pt 15):2710-2715.

44. Choi JW, Kim DG, Lee A-E, et al. Cancer-associated splicing variant of tumor suppressor AIMP2/p38: pathological implication in tumorigenesis. *PLoS Genetics*. 2011; 7(3):e1001351.

45. Choi JW, Lee J-W, Kim JK, et al. Splicing variant of AIMP2 as an effective target against chemoresistant ovarian cancer. *J Mol Cell Biol*. 2012;4(3):164-173.

46. Jung JY, Kim EY, Kim A, et al. Ratio of Autoantibodies of tumor suppressor AIMP2 and its oncogenic variant is associated with clinical outcome in lung cancer. *J Cancer*. 2017; 8(8):1347-1354.

47. Cao Q, Zhang J, Zhang T. AIMP2-DX2 promotes the proliferation, migration, and invasion of nasopharyngeal carcinoma cells. *BioMed Research International*. 2018;2018:9253036.

48. Yin K, Zhang Y, Zhang S, et al. Using weighted gene co-expression network analysis to identify key modules and hub genes in tongue squamous cell carcinoma. *Med UK Ed*. 2019; 98(37):e17100.

49. Coelho AI, Berry GT, Rubio-Gozalbo ME. Galactose metabolism and health. *Curr Opin Clin Nutr Metab Care*. 2015; 18(4):422-427.

50. Kathagen-Buhmann A, Maire CL, Weller J, et al. The secreted glycolytic enzyme GPI/AMF stimulates glioblastoma cell migration and invasion in an autocrine fashion but can have anti-proliferative effects. *Neuro Oncol*. 2018;20(12): 1594-1605.

51. Federzoni EA 1 is linking the glycolytic enzyme HK3 in neutrophil differentiation and survival of APL cells. *Blood*. 2012;119(21):4963-4970.

52. Favaro E, Bensaad K, Chong MG, et al. Glucose utilization via glycogen phosphorylase sustains proliferation and prevents premature senescence in cancer cells. *Cell Metabolism*. 2012; 16(6):751-764.

53. Yin W, Tang G, Zhou Q, et al. Expression profile analysis identifies a novel five-gene signature to improve prognosis prediction of glioblastoma. *Front Genet*. 2019;10:419.

54. Venkitachalam S, Revoredo L, Varadan V, et al. Biochemical and functional characterization of glycosylation-associated mutational landscapes in colon cancer. *Sci Rep*. 2016;6:23642.